J|A|C|S ARTICLES

Published on Web 06/07/2010

Formation and Reactivity of Chromium(V)−Thiolato Complexes: A Model for the Intracellular Reactions of Carcinogenic Chromium(VI) with Biological Thiols

Aviva Levina, Lianbo Zhang, and Peter A. Lay*

School of Chemistry, The University of Sydney, Sydney, New South Wales 2006, Australia

Received February 26, 2010; E-mail: peter.lay@sydney.edu.au

Abstract: The nature of the long-lived EPR-active Cr(V) species observed in cells and biological fluids exposed to carcinogenic Cr(VI) has been definitively assigned from detailed kinetic and spectroscopic analyses of a model reaction of Cr(VI) with *p*-bromobenzenethiol (RSH) in the presence or absence of cyclic 1,2-diols (LH_2) in aprotic or mixed solvents. The first definitive structures for Cr(V) complexes with a monodentate thiolato ligand, $[Cr^{V}O(SR)_4]^-$ ($g_{iso} = 1.9960$, $A_{iso} = 14.7 \times 10^{-4}$ cm^{-1}), $[Cr^{V}OL(SR)_2]^-$ ($g_{iso} = 1.9854$, $A_{iso} = (15.8-16.2) \times 10^{-4}$ cm^{-1}) and $[Cr^{V}(O)_2(SR)_2]^-$ ($g_{iso} = 1.9828$, $A_{iso} = 6.8 \times 10^{-4}$ cm^{-1}) were assigned by EPR spectroscopy and electrospray mass spectrometry. The unusually low A_{iso} (^{53}Cr) value for the latter species is consistent with its rare four-coordinate, bis-oxido structure. The $[Cr^{V}OL(SR)_2]^-$ species are responsible for the transient $g_{iso} \approx 1.986$ EPR signals observed in living cells and animals treated with Cr(VI) (where RSH and LH_2 are biological thiols and 1,2-diols, respectively). For the first time, concentrations of Cr(V) intermediates formed during the reduction of Cr(VI) were determined by quantitative EPR spectroscopy, and a detailed reaction mechanism was proposed on the basis of stochastic simulations of the kinetic curves for Cr(V) species. A key feature of the proposed mechanism is the regeneration of Cr(V) species in the presence of Cr(VI) through the formation of organic free radicals, followed by the rapid reactions of the formed radicals with Cr(VI). The concentration of Cr(V) grows rapidly at the beginning of the reaction, reaches a steady-state level, and then drops sharply once Cr(VI) is spent. Similar mechanisms are likely to operate during the reduction of Cr(VI) in biological environment rich in reactive C−H bonds, including the oxidative DNA damage by Cr(V) intermediates.

Introduction

Biological thiols, including glutathione (GSH, γ-Glu-Cys-Gly) and metallothioneins (small Cys-rich proteins) play a variety of physiological roles, including detoxification of heavy metal ions[1] such as Cr(VI), which is a recognized human carcinogen[2] and a major occupational and environmental hazard.[3] A crucial piece of evidence for the participation of thiols in Cr(VI) metabolism in cultured mammalian cells[4] and in the blood of Cr(VI)-treated animals[5] comes from the observation of a transient EPR signal at $g_{iso} \approx 1.986$, which has been assigned to Cr(V)−thiolato complexes based on the model studies[5,6] and on a decrease in the intensity of this signal in GSH-depleted cells.[4b] The transient Cr(V)−thiolato complexes are able to exchange ligands with ubiquitous biological 1,2-diols (carbohydrates and their derivatives), leading to long-lived Cr(V)−diolato complexes ($g_{iso} \approx 1.979$),[5−8] which are thought to be the key reactive species in Cr(VI)-induced genotoxicity and carcinogenicity.[6−9] Recent advances in the understanding of Cr(VI) reactions with biological thiols include structural characterization (by X-ray absorption spectroscopy) and detailed reactivity studies of Cr(V)−GSH[10] and Cr(VI)−GSH[11] complexes.

Due to the d^1 electronic structure of Cr(V) ions, EPR spectroscopy has long been used as a selective analytical technique for studies of Cr(V) intermediates formed during the reduction of Cr(VI) in biological and model systems,[7−9,12] but the difficulty in obtaining quantitative data from EPR spectra[8,12,13] complicates detailed kinetic and mechanistic studies on such systems. A method for the determination of Cr(V) concentration from EPR spectra, based on external calibration curves obtained for stable Cr(V) complexes (such as Na-$[Cr^{V}O(ehba)_2]$, where ehba = 2-ethyl-2-hydroxybutanoato)[14] has

(1) (a) Stefanidou, M.; Maravelias, C. *Curr. Top. Toxicol.* **2004**, *1*, 161–167. (b) Babu, G. N.; Ranjani, R.; Fareeda, G.; Murthy, S. D. S. *J. Phytol. Res.* **2007**, *20*, 1–6.
(2) International Agency for Research on Cancer (IARC). *Overall Evaluations of Carcinogenicity to Humans*. IARC, 2003. http://www.iarc.fr.
(3) Guertin, J., Jacobs, J. A., Avakian, C. P., Eds. *Chromium(VI) Handbook*; CRC Press: Boca Raton, 2005.
(4) (a) Levina, A.; Harris, H. H.; Lay, P. A. *J. Am. Chem. Soc.* **2007**, *129*, 1065–1075. (b) Borthiry, G. B.; Antholine, W. E.; Myers, J. M.; Myers, C. R. *J. Inorg. Biochem.* **2008**, *102*, 1449–1462.
(5) Sakurai, H.; Takechi, K.; Tsuboi, H.; Yasui, H. *J. Inorg. Biochem.* **1999**, *76*, 71–80.
(6) Levina, A.; Lay, P. A. *Coord. Chem. Rev.* **2005**, *249*, 281–298.
(7) (a) Signorella, S.; Palopoli, C.; Santoro, M.; Garcia, V.; Daier, V.; Gonzalez, J. C.; Roldan, V.; Frascaroli, M. I.; Rizzotto, M.; Sala, L. F. *Trends Inorg. Chem.* **2001**, *7*, 197–207. (b) Codd, R.; Irwin, J. A.; Lay, P. A. *Curr. Opin. Chem. Biol.* **2003**, *7*, 213–219.
(8) Levina, A.; Codd, R.; Lay, P. A. In *Biological Magnetic Resonance*; Hanson, G. R., Berliner, L. J., Eds.; Springer Publishers: New York, 2009; Vol. 28, Part 4, pp 551−579.
(9) (a) Sugden, K. D.; Stearns, D. M. *J. Environ. Pathol. Toxicol. Oncol.* **2000**, *19*, 215–230. (b) Levina, A.; Codd, R.; Dillon, C. T.; Lay, P. A. *Prog. Inorg. Chem.* **2003**, *51*, 145–250. (c) Codd, R.; Dillon, C. T.; Levina, A.; Lay, P. A. *Coord. Chem. Rev.* **2001**, *216−217*, 537–582.

10.1021/ja101675w

been proposed.[15] However, due to the sensitivity of EPR spectra to the position of the sample in the cavity of an EPR spectrometer, simultaneous measurements on the analyzed sample and the standard within the cavity are required for accurate calibration.[13] In this work, a simple way of obtaining quantitative results from EPR spectroscopy (placing two capillaries containing a reaction mixture and a standard Cr(V) solution into the same EPR tube) has been used for the first detailed kinetic study of the Cr(VI) reaction with a simple model thiol, *p*-bromobenzenethiol (RSH), in a variety of solvents, including mixed aqueous−organic systems. The reactions of the resultant Cr(V)−thiolato complexes with carbohydrate models (*cis*-1,2-cyclopentanediol and *cis*-1,2-cyclohexanediol)[7,12,16] were also studied to mimic the conditions of the formation of Cr(V)−diolato complexes in biological systems. The choice of the model thiol was determined by the following considerations: (i) apart from the thiolato S, there are no other potential donor atoms for Cr in the RSH molecule, which excludes the formation of chelated thiolato−Cr(V) species (unlike those for multifunctional ligands such as GSH and its derivatives);[10,17] (ii) the nonionic nature of RSH (as opposed to that of GSH and its derivatives)[10,17] and characteristic $^{79}Br/^{81}Br$ isotopic distribution patterns are beneficial for the studies of its Cr complexes by electrospray mass spectrometry (ESMS);[18] (iii) a stable and well-characterized Cr(VI)−thiolato complex, $(Ph_4As)[Cr^{VI}O_3(SR)]$,[11,19] can be used as a starting material for kinetic experiments; and (iv) RSH is relatively air-stable and nonvolatile and is easier to handle than other nonionic thiols. The only significant disadvantage of the RSH chosen for this research was its low water solubility. Preliminary studies of Cr(V) complexes formed in the reactions of Cr(VI) with *p*-bromobenzenethiol have been reported,[20] but no definitive characterization of these species has been achieved to date. Detailed information on the mechanisms of formation and decomposition of Cr(V)−RSH complexes, obtained in this work, has shed a new light on the nature of Cr(V) species formed during the reactions of Cr(VI) with biological thiols such as glutathione in vitro[10] as well as in cultured mammalian cells[4] and in living animals.[5]

Experimental Section

Caution! Cr(VI) compounds are human carcinogens,[2] and Cr(V) complexes are mutagenic and potentially carcinogenic;[9] appropriate precautions should be taken to avoid skin contact and inhalation of their solutions and dusts.

Reagents. Acetonitrile (MeCN) and *N*,*N*-dimethylformamide (DMF) (both of HPLC grade, Aldrich) were freshly distilled from activated molecular sieves (4 Å, Aldrich) before use. Other commercial reagents of analytical or higher purity (purchased from Aldrich, Sigma, or Merck) were used without further purification. Water was purified by the Milli-Q technique. The Cr(VI/V) complexes, $(Ph_4As)[Cr^{VI}(O)_3(SR)]$ (where RSH is *p*-bromobenzenethiol),[11,19] $Na[Cr^{V}O(ehba)_2]$,[14] $K[Cr^{V}OL_2]$ (where LH_2 = *cis*-1,2-cyclopentanediol or *cis*-1,2-cyclohexanediol),[16] and $K[Cr^{V}O(Aib_3-DMF)]$ (where Aib = 2-amino-2-methylpropanoic acid)[21] were synthesized and characterized as described previously. Attempts to isolate $[Cr^{V}O(SR)_4]^-$, based on the previously developed methods for the synthesis of Cr(V)−hydroximato[22] and −1,2-diolato[16] complexes, used the reaction of Cr(VI) (50 mM, from $(NH_4)_2Cr_2O_7$) with RSH (500 mM) in anhydrous DMF (0.50 mL) for 15 min at 295 K (optimal conditions for the formation of $[Cr^{V}O(SR)_4]^-$, see Results), followed by the addition of a mixture of *n*-hexane (5.0 mL) and anhydrous acetone (2.0 mL). The resultant dark, oily precipitate was separated by decanting the solvent and drying the residue under a stream of N_2. This procedure led to decomposition of $[Cr^{V}O(SR)_4]^-$ with the formation of $[Cr^{VI}(O)_3(SR)]^-$ and small amounts of $[Cr^{V}(O)_2(SR)_2]^-$, as shown by electrospray mass spectrometry (ESMS) and EPR spectroscopy (see Results). Previous attempts in the literature to isolate pure Cr(V)−RSH (RSH = *p*-bromobenzenethiol) complexes were also unsuccessful.[20]

Analytical Techniques. For EPR spectroscopy, freshly prepared and Ar-saturated stock solutions of Cr(VI) and RSH in DMF, DMSO (dimethylsulfoxide), or MeCN were mixed under an Ar atmosphere, and the mixture was transferred by a Hamilton syringe into quartz capillaries (length, 10 cm; internal diameter, 0.50 mm), which were then sealed from the top with vacuum grease. A capillary containing the reaction mixture was placed into a quartz EPR tube (length, 20 cm; internal diameter, 3 mm) together with a second capillary, containing a stable Cr(V) complex (0.050−2.0 mM $Na[Cr^{V}O(ehba)_2]$ in DMF solution, where ehba = 2-ethyl-2-hydroxybutanoato(2−)),[14] which was used as a concentration calibrant. All the preparations were carried out in dim light since both Cr(VI) and Cr(V) complexes are photosensitive.[16,23,24] Time-dependent EPR spectra (X-band) were collected on an Elexsys spectrometer (Bruker), equipped with an internal NMR gaussmeter, at 295 ± 1 K. Stock solutions of Cr(VI) complexes (20 mM of $(Ph_4As)[Cr^{VI}(O)_3(SR)]$ or 100 mM of $(NH_4)_2Cr_2O_7$ in DMF) and the calibration solutions of $Na[Cr^{V}O(ehba)_2]$ (0.050−2.0 mM) in DMF were stable for at least 12 h at 295 K when protected from light (determined by electronic absorption spectroscopy).[11,14] The validity of the calibration technique was confirmed by filling the two capillaries with DMF solutions of two stable Cr(V) complexes, $[Cr^{V}O(ehba)_2]^-$ and $[Cr^{V}O(Aib_3-DMF)]^-$,[21] at concentration ratios of 0.10−10; the ratios obtained from EPR spectral simulations were within 10% of the expected values (Figure S1 in Supporting Information). The g_{iso} value of $[Cr^{V}O(ehba)_2]^-$ (1.9777 in DMF solutions)[14d] was significantly lower than those of the Cr(V) species formed in the reaction mixtures (1.9790−1.9960, see Results), so that the calibrant signal did not interfere significantly with those of the measured Cr(V) species (typical examples are shown in Figure S2, Supporting Information). Spectral simulations with WinSim software[25] were used for the determination of Cr(V) concentrations, as well as of the g_{iso} and A_{iso} (^{53}Cr) values of the Cr(V) species (where second-order corrections were applied). Kinetic curves for Cr(V) species, obtained from the EPR spectral simulations, were modeled using Chemical Kinetics Simulator

(10) Levina, A.; Zhang, L.; Lay, P. A. *Inorg. Chem.* **2003**, *42*, 767–784.
(11) Levina, A.; Lay, P. A. *Inorg. Chem.* **2004**, *43*, 324–335.
(12) (a) Farrell, R. P.; Lay, P. A. *Comments Inorg. Chem.* **1992**, *13*, 133–175. (b) Barr-David, G.; Charara, M.; Codd, R.; Farrell, R. P.; Irwin, J. A.; Lay, P. A.; Bramley, R.; Brumby, S.; Ji, J.-Y.; Hanson, G. R. *J. Chem. Soc., Faraday Trans.* **1995**, *91*, 1207–1216.
(13) Mazur, M. *Anal. Chim. Acta* **2002**, *456*, 129–146.
(14) (a) Krumpolc, M.; Roček, J. *J. Am. Chem. Soc.* **1979**, *101*, 3206–3209. (b) Krumpolc, M.; Roček, J. *Inorg. Chem.* **1985**, *24*, 617–621. (c) Judd, R. J.; Hambley, T. W.; Lay, P. A. *J. Chem. Soc., Dalton Trans.* **1989**, 2205–2210. (d) Bramley, R.; Ji, J.-Y.; Judd, R. J.; Lay, P. A. *Inorg. Chem.* **1990**, *29*, 3089–3094.
(15) Chappell, J.; Chiswell, B.; Canning, A. *Talanta* **1998**, *46*, 23–38.
(16) Bartholomäus, R.; Irwin, J. A.; Shi, L.; Meejoo, S.; Levina, A.; Lay, P. A. *Inorg. Chem.* **2010**. Submitted.
(17) Zhang, L. EPR and XAFS Studies of Biologically Relevant Chromium(V) Complexes and Manganese(II)-Activated Aminopeptidase P. Ph.D. Thesis, The University of Sydney: Sydney, Australia, 1998.
(18) (a) Gaskell, S. J. *J. Mass Spectrom.* **1997**, *32*, 677–688. (b) Cole, R. B. *J. Mass Spectrom.* **2000**, *35*, 763–772.
(19) Mazurek, W.; Fallon, G. D.; Nichols, P. J.; West, B. O. *Polyhedron* **1990**, *9*, 777–779.
(20) Mazurek, W.; Nichols, P. J.; West, B. O. *Polyhedron* **1991**, *10*, 753–762.
(21) Barnard, P. J.; Levina, A.; Lay, P. A. *Inorg. Chem.* **2005**, *44*, 1044–1053.
(22) Gez, S.; Luxenhofer, R.; Levina, A.; Codd, R.; Lay, P. A. *Inorg. Chem.* **2005**, *44*, 2934–2943.
(23) Mitewa, M.; Bontchev, P. R. *Coord. Chem. Rev.* **1985**, *61*, 241–272.
(24) Bontchev, P. R.; Mitewa, M.; Russev, P.; Petrov, G.; Malinovski, A.; Kabassanov, K. *J. Inorg. Nucl. Chem.* **1979**, *41*, 1451–1456.
(25) Duling, D. R. *J. Magn. Reson.* **1994**, *B104*, 105–110. The *WinSim* software is available via the Internet at http://epr.niehs.nih.gov/.

software,[26] based on the stochastic approach (a typical number of reacting species in the simulations was 5×10^5).

The ESMS analyses were performed using a Finnigan LCQ mass spectrometer; typical experimental settings were as follows: sheath gas (N_2) pressure, 60 psi; spray voltage, 4.0 kV; capillary temperature, 473 K; cone voltage, 5 V; tube lens offset, 20 V; and *m*/*z* range, 100−2000 (both in negative- and positive-ion modes; no signals of Cr species were detected in the latter). Analyzed solutions (5 μL, 0.50 mM Cr in DMF) were injected into a flow of MeOH (flow rate, 0.30 mL min^{-1}). Acquired spectra were the averages of 10 scans (scan time, 10 ms). Simulations of the mass spectra were performed using IsoPro software.[27] Concentrations of unreacted RSH in the reaction mixtures after the complete reduction of Cr(VI) to Cr(III) were determined spectrophotometrically with Ellman's reagent,[28] as described previously.[29] Electronic absorption (UV−vis) spectroscopy was performed on a Hewlett-Packard HP 8452 A diode-array spectrophotometer (spectral range, 200−800 nm; resolution, 2.0 nm; acquisition time, 0.20 s). All the spectroscopic and kinetic measurements were performed at 295 ± 1 K.

Results

Reactions of Cr(VI) with RSH: Identification of Cr(V) Intermediates. On the basis of the results of previous studies of Cr(VI) reduction by glutathione in aqueous solutions,[10] the reaction of Cr(VI) with RSH was initially studied under the conditions that facilitated the detection and characterization of Cr(V) intermediates ([Cr(VI)] = 50 mM and [RSH] = 500 mM in DMF solutions at 295 K). The source of Cr(VI) in these experiments was $(NH_4)_2Cr_2O_7$, due to its higher solubility in DMF compared with those of the Na^+ or K^+ chromates or of $(Ph_4As)[CrO_3(SR)]$. The color of the reaction mixture changed within several minutes from orange to dark green. The reaction mixtures were diluted 100-fold with DMF at various time points, and electronic spectra of dilute solutions were recorded within ~30 s after the dilution (Figure S3a in Supporting Information). When the reaction mixture was diluted at an early stage (~30 s after mixing of the reagents), the resultant spectrum showed a characteristic absorbance band of $[Cr^{VI}O_3(SR)]^-$ (λ_{max} = 414 nm), which is different from that for a solution of $[Cr_2{}^{VI}O_7]^{2-}$ in DMF in the absence of RSH (λ_{max} = 380 nm) (Figure S3a [Supporting Information]).[11] This change was followed by the appearance of a broad absorbance band with $\lambda_{max} \approx$ 720 nm, which reached its maximal intensity at ~15 min after mixing of the reagents, and then decayed to the background level within the next ~70 min (Figure S3a). In other experiments, the reaction of Cr(VI) (50 mM) with RSH (500 mM) in DMF solution was allowed to proceed for 15 min at 295 K (to reach the maximum concentration for the intermediate with $\lambda_{max} \approx$ 720 nm), then the reaction mixtures were diluted 100-fold with DMF, and time-dependent absorbance changes (295 K) in dilute solutions were followed by electronic absorption spectroscopy (Figure S3b in Supporting Information). In these experiments, the intensity of absorbance at ~720 nm decayed to the background level within ~60 min, and a shoulder at ~414 nm appeared, which was indicative of the presence of $[Cr^{VI}(O)_3(SR)]^-$.[11]

Undiluted reaction mixtures ($[Cr(VI)]_0$ = 50 mM and $[RSH]_0$ = 500 mM in DMF solution at 295 K) showed a single isotropic EPR signal of a Cr(V) intermediate (Figure 1a; g_{iso} = 1.9960; $A_{iso}(^{53}Cr) = 14.7 \times 10^{-4}$ cm^{-1}). A marked decrease in the linewidths of the ^{53}Cr satellite signals with an increase in magnetic field was observed for this species (inset in Figure 1a). All these signals (designated with asterisks in Figure 1a) were of the same integral intensity (within 10% experimental error, as determined by EPR spectral simulations), so these signals were due to the ^{53}Cr satellites of the main Cr(V) species (g_{iso} = 1.9960), and not due to the other minor Cr(V) species.

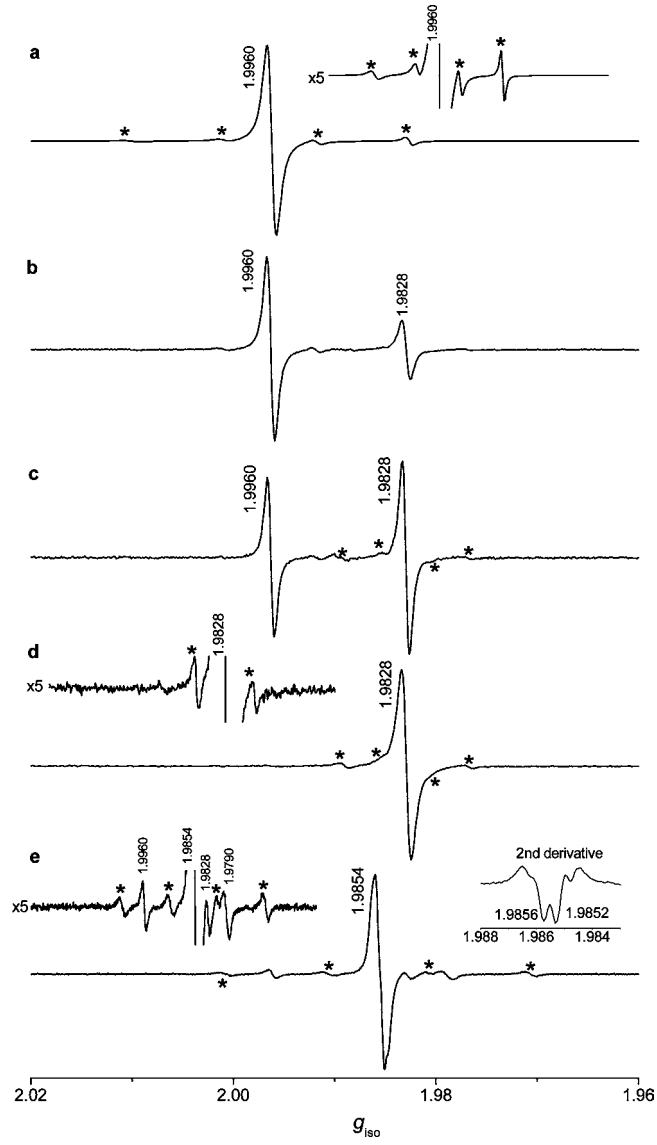

Figure 1. Typical EPR spectra (X-band, 295 K) of Cr(V) species formed during the reactions of Cr(VI) ($(NH_4)_2Cr_2O_7$, a−d) or Cr(V) ($K[Cr^VO(cpd)_2]$, where cpd = *cis*-1,2-cyclopentanediol,[16] (e) complexes with *p*-bromobenzenethiol (RSH) in DMF solutions. All the reactions were performed at 295 K, and the spectra were collected in the absence of a Cr(V) standard (see the Experimental Section). Signals due to the ^{53}Cr hyperfine splitting[8,12] are designated with asterisks. Reaction conditions: (a) Cr(VI) (50 mM) reacted with RSH (500 mM) in DMF for ~3 min, undiluted reaction mixture; (b) Cr(VI) (50 mM) reacted with RSH (500 mM) in DMF for 15 min, then the reaction mixture was diluted 100-fold with DMF, and the spectrum was collected at 5 min after the dilution; (c) same as (b), but 15 min after the dilution; (d) Cr(VI) (50 mM) reacted with RSH (500 mM) in DMF for 15 min, then the Cr(V) complexes were precipitated by a mixture of hexane and acetone (see the Experimental Section) and redissolved in DMF at [Cr] ~ 10 mM, the spectrum was recorded at ~3 min after the dissolution in DMF; and (e) Cr(V) (0.50 mM) reacted with RSH (10 mM) in DMF for ~3 min, undiluted reaction mixture.

(26) (a) *Chemical Kinetics Simulator, Version 1.01*; IBM Almaden Research Center, New York, 1996, http://www.almaden.ibm.com/st/computational_science/ck/?cks; (b) Levina, A.; Lay, P. A.; Dixon, N. E. *Inorg. Chem.* **2000**, *39*, 385–395.
(27) Senko, M. *IsoPro 3.0*; Freeware, 1998.
(28) Ellman, G. L. *Arch. Biochem. Biophys.* **1959**, *82*, 70–77.
(29) Levina, A.; Bailey, A. M.; Champion, G.; Lay, P. A. *J. Am. Chem. Soc.* **2000**, *122*, 6208–6216.

Table 1. Mass Spectrometric and EPR Spectroscopic Data for Cr Intermediates Detected During the Reactions of Cr(VI) or Cr(V) with *p*-Bromobenzenethiol and a Cyclic Diol[a]

species[b]	$-m/z$[c]	g_{iso}	A_{iso}[d] $\times 10^{-4}$ cm^{-1}
$[Cr^{V}(O)_2(SR)_2]^-$	460.1	1.9828	6.8
$[Cr^{V}O(SR)_4]^-$	820.0	1.9960	14.7
$[Cr^{V}O(cpd)(SR)_2]^-$	543.7	1.9852 (60%)[e]	15.8[e]
		1.9856 (40%)[e]	
$[Cr^{V}O(chd)(SR)_2]^-$	557.9	1.9853 (50%)[e]	16.2[e]
		1.9855 (50%)[e]	
$[Cr^{VI}(O)_3(SR)]^-$	287.1	−	−
$[Cr^{IV}O(SR)_3]^-$[f]	631.1	−	−
$[Cr^{III}(SR)_4]^-$[f]	804.0	−	−

[a] Reaction conditions corresponded to those described in the captions to Figures 1 and 2. [b] Designations of ligands: RSH = *p*-bromobenzenethiol; $cpdH_2$ = *cis*-1,2-cyclopentanediol; and $chdH_2$ = *cis*-1,2-cyclohexanediol. [c] Values for the highest peak in the isotopic distribution (Figures 2 and S4). [d] Hyperfine splitting due to the ^{53}Cr nuclei ($S = 3/2$; natural abundance, 9.55%).[12] [e] The EPR signals were simulated for a mixture of two geometric isomers;[7,16] the A_{iso} values were similar for both isomers and were not resolved. [f] These species were only observed under ESMS conditions; the Cr(IV) and Cr(III) species in solutions are likely to bind solvent molecules as extra ligands.[18]

The intensity of the $g_{iso} = 1.9960$ signal increased within ~15 min and then decreased to zero within ~80 min after mixing of the reagents, in accordance with the changes in the absorbance intensity at ~720 nm (Figure S3a [Supporting Information]). Dilution of the reaction mixture (100-fold with DMF) led to the appearance and growth of a second EPR signal ($g_{iso} = 1.9828$; Figure 1b,c). On the basis of the electronic absorption and EPR spectroscopic data (Figures 1 and S3 [Supporting Information]), isolation of the main Cr(V) intermediate ($g_{iso} = 1.9960$) from the concentrated reaction mixture was attempted by a method previously used for the isolation of Cr(V)−hydroximato and −1,2-diolato complexes[16,22] (see the Experimental Section). The resultant black powder was dissolved in DMF ([Cr] ~ 10 mM), and the EPR spectrum of the solution showed only the $g_{iso} = 1.9828$ signal (Figure 1d), which had an unusually low $A_{iso}(^{53}Cr)$ value[12] for a Cr(V) complex (6.8×10^{-4} cm^{-1}; inset in Figure 1d). The EPR spectroscopic parameters of the Cr(V) species are summarized in Table 1.

The conditions used for the ESMS experiments corresponded to those used for the electronic absorption and EPR spectroscopic measurements (Figures 1 and S3 [Supporting Information]; $[Cr(VI)]_0 = 50$ mM and $[RSH]_0 = 500$ mM in DMF solutions at 295 K), including dilutions (100-fold with DMF) of the reaction mixtures at various time points, followed by immediate collection of the spectra, as well as the studies of time-dependent changes in dilute reaction mixtures. Typical ESMS data are shown in Figure 2 and Figure S4, Supporting Information, and the $-m/z$ values of major Cr species are summarized in Table 1. At ~30 s after mixing of the reagents, the dominant ESMS signal was due to $[Cr^{VI}(O)_3(SR)]^-$ ($m/z = -287.3$; Figure S4a [Supporting Information] and Table 1).[11] As the reaction progressed, the signal of $[Cr^{V}O(SR)_4]^-$ ($m/z = -820.0$; Table 1) became more abundant, reaching its maximal intensity at ~15 min after initiation of the reaction (Figure 2a). The spectrum in Figure 2a was collected within ~30 s after dilution of the reaction mixture. When the dilute reaction mixtures were left at 295 K for a longer time, the signals of $[Cr^{VI}O_3(SR)]^-$ and $[Cr^{V}(O)_2(SR)_2]^-$ ($m/z = -460.1$; Table 1) grew on the expense of that of $[Cr^{V}O(SR)_4]^-$ (see Figure S4b, time after dilution 10 min; and Figure 2b, time after dilution 40 min), in parallel with the relative growth of the $g_{iso} = 1.9828$ signal in EPR spectra under the same conditions (Figure 1b,c). The growth and decay of the $[Cr^{V}O(SR)_4]^-$ signal in ESMS were accompanied by corresponding changes of the $[Cr^{IV}O(SR)_3]^-$ signal ($m/z = -633.1$; Table 1 and Figures 2a and S4a,b [Supporting Information]). This Cr(IV) species is likely to form from reduction of $[Cr^{V}O(SR)_4]^-$ under the conditions of negative-ion ESMS,[18] as shown by their roughly constant abundance ratio (25−35% Cr(IV) relative to Cr(V)) at a low cone voltage (−5 V; Figures 2a and S4a,b [Supporting Information]), and by a marked increase in the relative abundance of the Cr(IV) species at a high cone voltage (−100 V; Figure S4c [Supporting Information]). When the reaction was allowed to proceed for ~60 min prior to the dilution, most of the signals due to the Cr(VI/V/IV) species had disappeared, and a weak signal appeared due to a Cr(III) species ($[Cr^{III}(SR)_4]^-$; $m/z = -804.0$; Table 1 and Figure S4d [Supporting Information]). Finally, the black solid isolated from the concentrated reaction

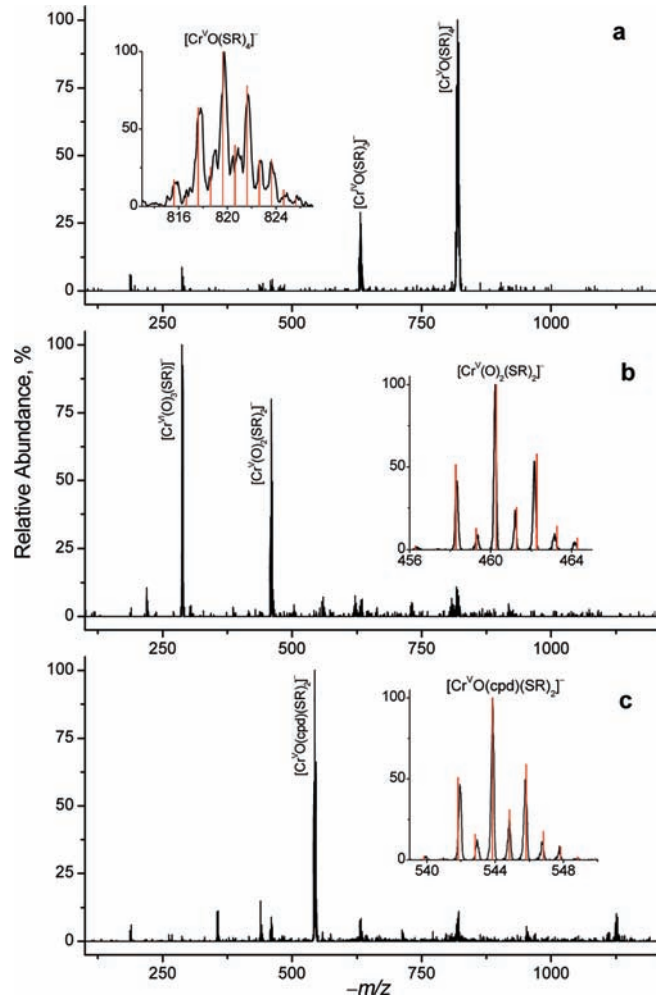

Figure 2. Typical ESMS data (see the Experimental Section for instrumental parameters) for the reactions of Cr(VI) ($(NH_4)_2Cr_2O_7$, a,b) or Cr(V) ($K[Cr^{V}O(cpd)_2]$, where cpd = *cis*-1,2-cyclopentanediol);[16] (c) complexes with *p*-bromobenzenethiol (RSH) in DMF solutions at 295 K (see also Figure S4 in Supporting Information). A summary of the *m*/*z* values for major Cr species is given in Table 1. Experimental (black lines) and simulated[27] (red columns) isotopic distributions of the Cr(V) signals are shown in the insets. Reaction conditions: (a) Cr(VI) (50 mM) reacted with RSH (500 mM) in DMF for 15 min, then the reaction mixture was diluted 100-fold with DMF, and the spectrum was collected at ~30 s after the dilution; (b) same as (a), but 40 min after the dilution; (c) Cr(V) (0.50 mM) reacted with RSH (10 mM) in DMF for ~3 min, undiluted reaction mixture.

mixture (see the Experimental Section), after dissolution in DMF ([Cr] ~ 1 mM) showed a main signal due to $[Cr^{VI}(O)_3(SR)]^-$ and a minor one due to $[Cr^{V}(O)_2(SR)_2]^-$ (no detectable levels of $[Cr^{V}O(SR)_4]^-$; Figure S4e [Supporting Information]), in agreement with the presence of only one Cr(V) signal in the corresponding EPR spectrum ($g_{iso} = 1.9828$, Figure 1d). Typical experimental and calculated isotopic distributions in the ESMS signals of Cr(V) complexes (arising from the roughly equal abundance of ^{79}Br and ^{81}Br isotopes in the ligand)[27] are shown in the insets within Figure 2.

In summary, two Cr(V) intermediates have been identified (by a combination of electronic absorption and EPR spectroscopies and ESMS) during the reduction of Cr(VI) by excess RSH in DMF solutions: $[Cr^{V}O(SR)_4]^-$, ($m/z = -820.0$; $g_{iso} = 1.9960$; $A_{iso}(^{53}Cr) = 14.7 \times 10^{-4}$ cm^{-1}; λ_{max} ~720 nm), which is predominantly formed at high concentrations of the reagents; and $[Cr^{V}(O)_2(SR)_2]^-$ ($m/z = -460.1$; $g_{iso} = 1.9828$; $A_{iso}(^{53}Cr) = 6.8 \times 10^{-4}$ cm^{-1}; no distinct absorbance peaks at 400−800 nm), which is formed on dilution of the reaction solutions with excess DMF or at an attempted isolation of $[Cr^{V}O(SR)_4]^-$. These spectral features were then used in the identification and quantification of intermediates in the kinetic studies.

Kinetic Experiments and Modeling. Detailed kinetic studies of the Cr(VI) reduction by RSH (focused on the formation and decay of Cr(V) species) were carried out by quantitative EPR spectroscopy at 295 K, using $Na[Cr^{V}O(ehba)_2]$ (0.050−2.0 mM solutions in DMF) as an internal standard (see the Experimental Section). Two parallel experimental series were carried out using either $(Ph_4As)[Cr^{VI}(O)_3(SR)]$[11,19] or $(NH_4)_2Cr_2O_7$ as the sources of Cr(VI), with $[Cr(VI)]_0 = 1.0-10$ mM and $[RSH]_0 = 20-750$ mM, in DMF, DMSO, MeCN, or mixed solvents (DMF/H_2O or DMF/MeOH; a full list of kinetic experiments is given in Table S1, Supporting Information). In the experiments using $[Cr_2^{VI}O_7]^{2-}$ as a source of Cr(VI), the initial concentration of RSH was increased by the value of $[Cr(VI)]_0$, to allow for the formation of $[Cr^{VI}(O)_3(SR)]^-$.[11] Under the studied reaction conditions, the choice of the Cr(VI) source did not significantly affect the reaction kinetics. Kinetic data for all the reaction conditions listed in Table S1 (including the use of alternative sources of Cr(VI)) are shown in Figure S5, Supporting Information.

The most prominent feature of the reactions of Cr(VI) (10 mM) with excess RSH (≥50 mM) in DMF or DMSO solutions was the rapid formation of the $g_{iso} = 1.9960$ species ($[Cr^{V}O(SR)_4]^-$, Table 1) followed by a period of a steady-state concentration and then by a rapid decay (solid black and red lines in Figure 3, and red line in Figure 4a). This unusual kinetic behavior was confirmed by electronic spectroscopy (using the specific absorbance of $[Cr^{V}O(SR)_4]^-$ at 720 nm, Figure S3 [Supporting Information]); a comparison of typical kinetic curves obtained by the both methods is shown in Figure S6, Supporting Information. Previously, similar kinetic behavior was observed (but not explained) by Roček and co-workers[30] for Cr(V) species (detected by their specific absorbance at ~750 nm) that are formed during the reactions of Cr(VI) with 2-hydroxycarboxylic acids in acidic aqueous solutions. In the current work, since $[Cr^{V}(O)_2(SR)_2]^-$ (unlike $[Cr^{V}O(SR)_4]^-$) did not show any characteristic absorbance peaks (see above), there was no alternative to the use of EPR spectroscopy for detailed studies of the formation and decay of both of the Cr(V) intermediates. In addition, unlike most of the previous kinetic studies of Cr(VI) reduction,[30,31] electronic absorption spectroscopy could not be used to follow the changes in concentrations of Cr(VI) species, since their absorbance at ~400 nm was masked by that of the excess ligand and Cr(V) species (Figure S3, Supporting Information).

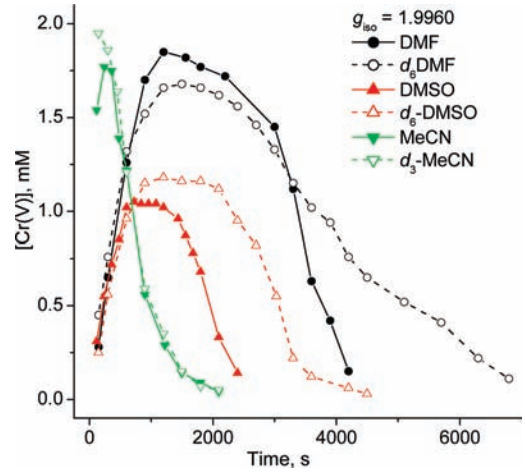

Figure 3. Typical kinetic curves for the formation of $[Cr^{V}O(SR)_4]^-$ ($g_{iso} = 1.9960$) species in deuterated and undeuterated solvents during the reactions of $[Cr^{VI}(O)(SR)_3]^-$ (10 mM) with RSH (250 mM) at 295 K, as observed by quantitative EPR spectroscopy with $Na[Cr^{V}O(ehba)_2]$ as an internal standard (see the Experimental Section for details). A full set of kinetic curves for all the reaction conditions listed in Table 2 is given in the kinetic curves for the reactions in mixed solvents (DMF/H_2O or DMF/MeOH) shown in Figure S5, Supporting Information.

In contrast to the reactions in DMF or DMSO solutions, the kinetics of the formation and decay of Cr(V) species in the reactions of Cr(VI) with a large excess of RSH in MeCN solutions were close to those for typical sequential pseudo-first-order reactions[6,31] (solid green line in Figure 3). The use of deuterated MeCN did not significantly alter the reaction kinetics compared with that in the undeuterated solvent, in contrast to the major differences in the reaction kinetics in deuterated vs undeuterated DMF or DMSO (dashed lines in Figure 3). Addition of protic solvents such as H_2O (5−20% vol/vol) or MeOH (10−65% vol/vol) to the reaction solutions (10 mM Cr(VI) and 250 mM RSH) in DMF caused the Cr(V) intermediate ($[Cr^{V}O(SR)_4]^-$, $g_{iso} = 1.9960$) to form and decay more rapidly, without major changes in the maximal amounts of resultant Cr(V) (rows 21−27 in Table S1 and the corresponding data in Figure S5, Supporting Information). The $g_{iso} = 1.9960$ value for $[Cr^{V}O(SR)_4]^-$ was solvent independent. Higher concentrations of H_2O could not be used because of precipitation of RSH, and the reactions in pure MeOH were too fast to monitor the formation and decay of Cr(V) intermediates by EPR spectroscopy. The minimal amount of H_2O added to DMF in the mixed-solvent studies (5% vol/vol or ~3 M) was at least 2 orders of magnitude higher than the amounts of H_2O expected to form in the redox reaction (30 mM from 10 mM Cr(VI), Scheme 1) or to be present in dried and freshly distilled DMF (<10 mM).[32]

The most simple scheme that adequately describes the observed kinetic phenomena (obtained by the stochastic simula-

(30) (a) Krumpolc, M.; Roček, J. *J. Am. Chem. Soc.* **1977**, *99*, 137–143. (b) Mahapatro, S. N.; Krumpolc, M.; Roček, J. *J. Am. Chem. Soc.* **1980**, *102*, 3799–3806.

(31) Lay, P. A.; Levina, A. *Inorg. Chem.* **1996**, *35*, 7709–7717.

(32) Izutsu, K. *Electrochemistry in Nonaqueous Solutions*; Wiley-VCH: Weinhem, Germany, 2002; pp 85−106 and 287−300.

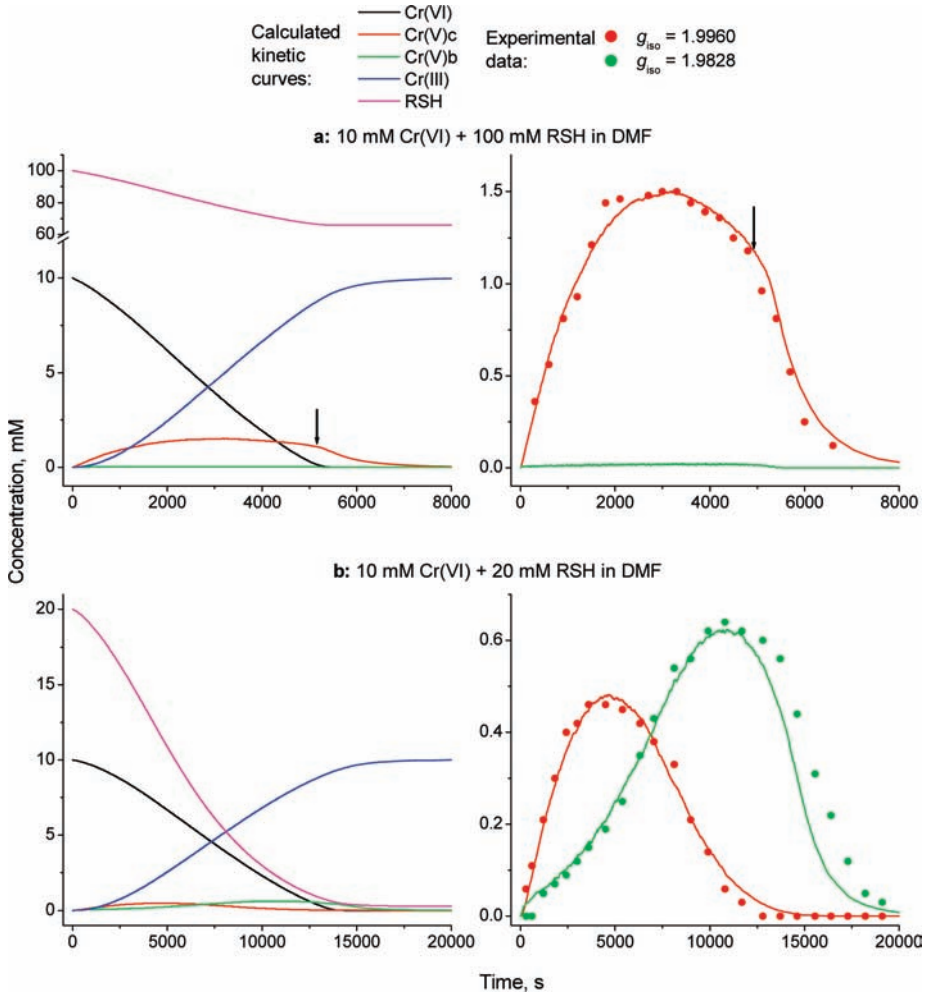

Figure 4. Typical experimental and calculated[26] kinetic curves for the reaction of $[Cr^{VI}O_3(SR)]^-$ (10 mM) with RSH (a, 100 mM or b, 20 mM) in DMF solutions at 295 K. The experimental data were obtained by quantitative EPR spectroscopy with $Na[Cr^{V}O(ehba)_2]$ as an internal standard (see the Experimental Section). The kinetic model and designations of the reacting species correspond to Table 2. Expanded views (a, Right) and (b, Right) of experimental (filled circles) and calculated (lines) kinetic curves for the Cr(V) species (the species giving rise to the $g_{iso} = 1.9828$ signal were not detected at $[RSH]_0 = 100$ mM). The arrows in (a) show the time point when a rapid decay of Cr(V) begins, corresponding to the disappearance of Cr(VI).

tion method)[26] is shown in Table 2 (eqs 1−8), and the values of the rate constants that were dependent on the reaction conditions (k_1, k_4, and k_6) are listed in Table S1 (Supporting Information) (the other rate constants are given in Table 2). Typical examples of calculated kinetic curves for the main reacting species, as well as experimental kinetic curves for Cr(V) species present during the reactions of Cr(VI) (10 mM) with high or low concentrations of RSH (100 or 20 mM, respectively), are shown in Figure 4a and b. A comparison of experimental and calculated kinetic curves (for Cr(V) species only) for all the reaction conditions used (see Table S1 [Supporting Information]) is shown in Figure S5, and a comparison of calculated kinetic curves for Cr(V) species under various reaction conditions is given in Figure S7 (Supporting Information). Many alternative kinetic schemes were considered and rejected, since they failed to reproduce the observed dependences of the kinetic curves for Cr(V) intermediates on the reaction conditions (typical examples are shown in Table S2 and Figure S8, Supporting Information).

Since all the reactions were performed in the presence of excess RSH over Cr(VI) (see Table S1 [Supporting Information]) and no kinetic differences were observed when either $[Cr^{VI}(O)_3(SR)]^-$ or $[Cr_2{}^{VI}O_7]^{2-}$ was used as a source of Cr(VI) (Figure S5 [Supporting Information]), $[Cr^{VI}(O)_3(SR)]^-$ was assumed to be the only reactive form of Cr(VI).[11] According to the proposed kinetic scheme (Table 2), the first Cr(V) intermediate formed by one-electron reduction of Cr(VI) (designated as Cr(V)a, eq 1 in Table 2) was unstable and was not detected by EPR spectroscopy (its calculated concentrations never exceeded 2% of the total Cr(V) concentration). Further reactions of Cr(V)a with excess RSH (eqs 2 and 3 in Table 2) produced two relatively stable Cr(V) species, designated as Cr(V)b and Cr(V)c that correspond to $[Cr^{V}(O)_2(SR)_2]^-$ and $[Cr^{V}O(SR)_4]^-$, respectively, (see the Discussion section for details). These species reacted with solvents, such as DMF or DMSO, to produce free radicals (designated as Solv$^{\bullet}$; eqs 4 and 7 in Table 2), which then rapidly reacted with Cr(VI) to regenerate Cr(V) species (eq 5 and 7 in Table 2). The ability of DMF to form radicals on the reactions with oxidants, including Cr(V), has been reported previously.[21,33] These reactions led to relatively constant levels of Cr(V) species in the reaction mixtures in the presence of excess Cr(VI), and to their rapid decay when Cr(VI) was spent (see the representative calculated kinetic curves in Figure 4a). The same relation between the kinetic curves for Cr(VI) and Cr(V) species formed in the reactions of Cr(VI) with 2-hydroxycarboxylic acids in acidic

(33) Muzart, J. *Tetrahedron* **2009**, *65*, 8313–8323.

Scheme 1. Proposed Mechanism for the Cr(VI) + RSH Reaction (Equation Numbers and Designations of the Reacting Species Correspond to Those in Table 2)[a]

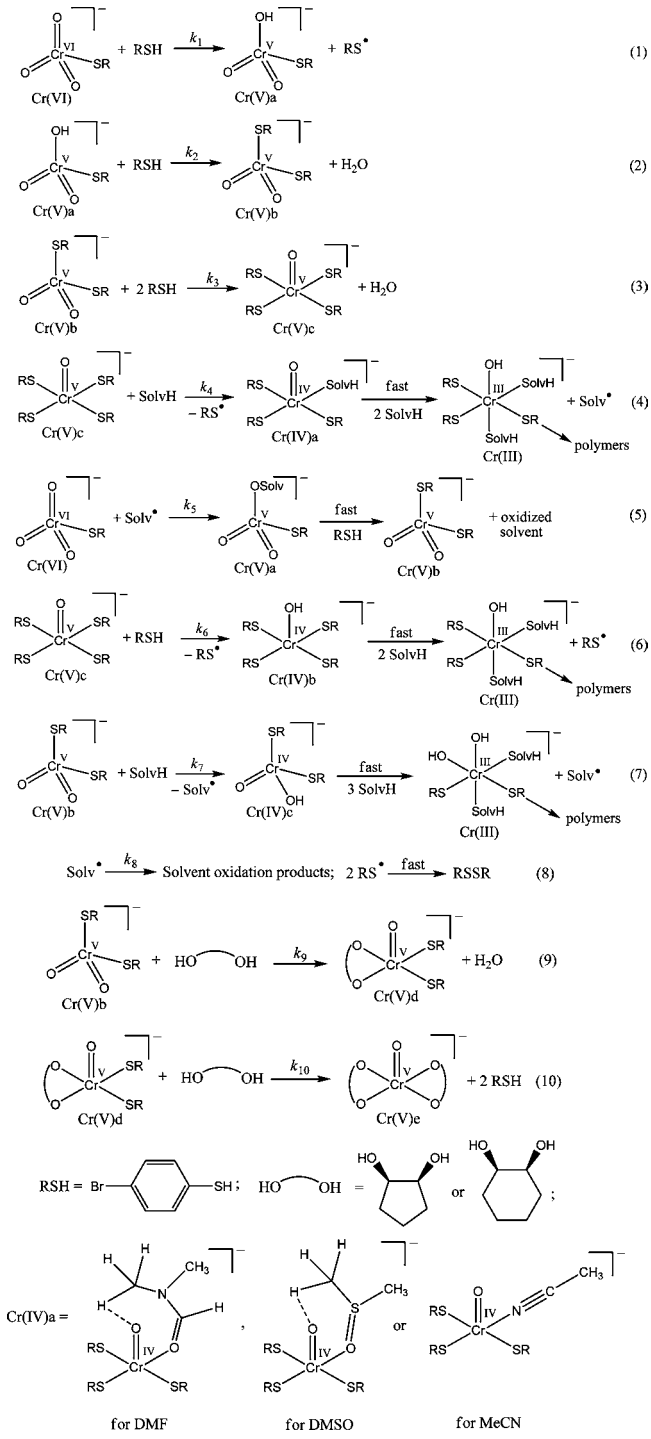

[a] Some alternative variants of the mechanism, rejected on the basis of kinetic analysis, are shown in Table S1 and Scheme S1, Supporting Information.

aqueous media was observed by Roček and co-workers,[30] who calculated these curves from electronic absorption spectra. The rest of the proposed kinetic scheme consisted of the reduction of Cr(V)c to a Cr(III) product by excess RSH, and quenching of the Solv• radicals (eqs 6 and 8 in Table 2).

The observed deuterium kinetic isotope effect (KIE = k_{4H}/k_{4D}) values for the reactions of Cr(V)c with DMF (1.7) or DMSO (2.3) solvents (see Figure 3 and the k_4 values for the corresponding reactions in Table S1 [Supporting Information]) are consistent with the production of Solv• radicals during the reactions of C−H bonds of the solvent molecules with Cr(V). The corresponding reactions in MeCN solutions were at least an order magnitude slower than those in DMF or DMSO solutions (see the k_4 values in rows 17−20, Table 2), which was consistent with much lower reactivity MeCN toward oxidants compared with DMF or DMSO. For instance, electrochemical oxidation of MeCN occurs at +3.0 V vs +1.5 V for both DMF and DMSO (using the ferricenium/ferrocene couple as a reference).[32] Changes in the reaction kinetics caused by the addition of H_2O or MeOH to DMF solutions were modeled by the increases in the rate constants k_1 and k_4 (Table S1 [Supporting Information]). The calculated values of k_4 also increased at very high concentrations of RSH (≥500 mM, Table S1 [Supporting Information]), which pointed to a change in the reaction mechanism under these conditions. The reaction kinetics at low RSH concentrations (≤20 mM at $[Cr(VI)]_0$ = 10 mM) could not be described adequately by the scheme in Table 2, probably because of the participation of more than one form of Cr(VI) (e. g., $[Cr^{VI}(O)_3SR]^-$ and $[HCr^{VI}O_4]^-$).[11] Detailed studies of the reaction kinetics at very high or very low RSH concentrations were beyond the scope of the current work, since these conditions were not relevant to the biological context of the reactions of interest.[4,6]

The involvement of solvents in the redox reactions (eqs 4, 6 and 7 in Table 2) led to the solvent-dependence of the reaction stoichiometry, with the amount of RSH required for the complete reduction of Cr(VI) to Cr(III) being generally lower (by about one molar equivalent) in DMF solutions compared with MeCN solutions (Figure S9 in Supporting Information). The observed reaction stoichiometry (2−5 mols of RSH required for the reduction of one mol of $[Cr^{VI}(O)_3(SR)]^-$ to Cr(III) products) was also dependent on the initial concentration of RSH (due to the various proportions of the two main Cr(V) intermediates being formed), as confirmed by kinetic modeling (Figure S9 [Supporting Information]).

The determination of Cr(V) concentrations during the reactions of Cr(VI) with RSH (by quantitative EPR spectroscopy) showed that under no conditions did the total concentration of Cr(V) intermediates exceed 20% (mol.) of the initial concentration of Cr(VI) (Figure S5). This finding was supported by the results of kinetic modeling (e.g., Figure 4), which taken together, suggest that Cr(V) species always coexist in the reaction mixtures with larger amounts of Cr(VI) and Cr(III) species. Therefore, these reactions could not be used for quantitative generation of Cr(V) thiolato complexes in solutions for structural studies by X-ray absorption spectroscopy (in contrast to our previous studies of reactive Cr(VI/V/IV) complexes).[10,11,34] Note that ESMS data (Figure 2a) suggested a higher yield of $[Cr^VO(SR)_4]^-$, possibly due to the higher sensitivity of the ion detector to this species compared with that for $[Cr^{VI}(O)_3(SR)_4]^-$. An attempted isolation of the $[Cr^VO(SR)_4]^-$ complex (see the Experimental Section) led to its decomposition (Figures 1d and S4e [Supporting Information]).

Reactions of Cr(V) Thiolato Complexes in Dilute Solutions and Ligand-Exchange Reactions with 1,2-Diols. In order to determine the possible fate of Cr(V) thiolato intermediates in biological media, the reactivities of Cr(V)−thiolato complexes were studied under the conditions that were used previously

(34) Levina, A.; Codd, R.; Foran, G. J.; Hambley, T. W.; Maschmeyer, T.; Masters, A. F.; Lay, P. A. *Inorg. Chem.* **2004**, 1046–1055.

Table 2. Proposed Kinetic Model for the Reaction of Cr(VI) with Excess RSH at 295 K[a]

reaction[b]		rate constant
Cr(VI) + RSH → Cr(V)a	(1)	$k_1 = (1-10) \times 10^{-3}$ M^{-1} s^{-1} [c]
Cr(V)a + RSH → Cr(V)b	(2)	$k_2 \geq 2$ M^{-1} s^{-1}
Cr(V)b + 2 RSH → Cr(V)c	(3)	$k_3 = 20 \pm 5$ M^{-2} s^{-1}
Cr(V)c + 2 SolvH[d] → Cr(III) + 2 Solv$^{\bullet}$	(4)	$k_4 = (0-10) \times 10^{-3}$ s^{-1} [c]
Cr(VI) + Solv$^{\bullet}$ → Cr(V)a	(5)	$k_5 \geq 250$ M^{-1} s^{-1}
Cr(V)c + RSH+SolvH[d] → Cr(III)	(6)	$k_6 = (3-30) \times 10^{-3}$ M^{-1} s^{-1} [c]
Cr(V)b + 2 SolvH[d] → Cr(III) + 2 Solv$^{\bullet}$	(7)	$k_7 = (1.0 \pm 0.2) \times 10^{-3}$ s^{-1}
Solv$^{\bullet}$ → oxidized solvent	(8)	$k_8 \geq (2.0 \pm 0.2) \times 10^{-3}$ s^{-1}
Cr(V)b + LH_2 → Cr(V)d[e]	(9)	$k_9 = (6 \pm 2) \times 10^{-3}$ M^{-1} s^{-1};[f,h] $(1.0 \pm 0.3) \times 10^{-3}$ M^{-1} s^{-1};[g,h] or $(5 \pm 0.6) \times 10^{-2}$ M^{-1} s^{-1} [f,i]
Cr(V)d + LH_2 → Cr(V)e[e]	(10)	$k_{10} = (2.0 \pm 0.5) \times 10^{-4}$ M^{-1} s^{-1}; [f,g,h] or $(1.0 \pm 0.07) \times 10^{-2}$ M^{-1} s^{-1} [f,i]

[a] The most simple kinetic model (see Scheme 1 for details) that adequately describes the kinetics of formation and decomposition of Cr(V) species under the conditions listed in Table S1 (Supporting Information), using either $(Ph_4As)[Cr^{VI}(O)_3(SR)]$ or $(NH_4)_2Cr_2O_7$ as a source of Cr(VI) (see Figure S5, Supporting Information, for comparison of the experimental and calculated kinetic curves). Representative alternative models are shown in Table S2 and Scheme S1, Supporting Information. [b] Equation numbers (in parentheses) and designations of the reaction intermediates correspond to Scheme 1. [c] The value of the rate constant is solvent-dependent, see Table S1 [Supporting Information] for details. [d] SolvH = solvent molecule (e.g., DMF). Concentrations of the solvents were assumed to be constant in the kinetic analysis. [e] Ligand-exchange reactions with large excesses of 1,2-diolato ligands, see Scheme 1. [f] For LH_2 = *cis*-1,2-cyclopentanediol ($cpdH_2$). [g] For LH_2 = *cis*-1,2-cyclohexanediol ($chdH_2$). [h] In DMF solution. [i] In DMF/H_2O (4:1 vol/vol) solution.

for identification of the reaction intermediates (Figures 1, 2, S3 and S4 [Supporting Information]). Namely, the $[Cr^{V}O(SR)_4]^-$ complex was generated by the reaction of Cr(VI) (50 mM, from $(NH_4)_2Cr_2O_7$) with RSH (500 mM) in DMF solutions (reaction time 15 min at 295 K, Figure S3a [Supporting Information]), then the reaction mixtures were diluted 100-fold with various solvents, and the decomposition of Cr(V) was followed by quantitative EPR spectroscopy. Concentrations of all of the reacting species at the time point of dilution were calculated from the kinetic model (Table 2). A good correspondence between calculated and experimental values of Cr(V) concentrations under these conditions is shown in Figure S5 (data set 13 [Supporting Information]). The calculated concentration values for all the reacting species were then divided by the factor of 100 (to account for the dilution) and used to calculate the kinetic profiles for Cr(V) species in dilute solutions from the same kinetic model (typical examples are shown in Figure 5 and Figure S10, Supporting Information). For instance, Figure 5a shows a good correspondence between the experimental and calculated kinetic curves for the decay of Cr(V)c ($[Cr^{V}O(SR)_4]^-$, $g_{iso} = 1.9960$) and the growth and decay of Cr(V)b ($[Cr^{V}(O)_2(SR)_2]^-$, $g_{iso} = 1.9828$) in a dilute solution. By contrast, direct reactions of low concentrations of Cr(VI) and RSH (0.50 and 5.0 mM, respectively, to approximate the conditions in the dilute reaction mixture) in DMF solutions led to negligibly slow formation of Cr(V) intermediates, as confirmed by kinetic modeling using the parameters contained in Tables S1 and 2 (Figure S10a). Experimentally, no $g_{iso} = 1.9960$ species and only marginal concentrations of the $g_{iso} = 1.9828$ species could be detected under these conditions (Figure S10a).

Reactions of the preformed $[Cr^{V}O(SR)_4]^-$ species with DMF solutions containing various concentrations of cyclic 1,2-diols (*cis*-1,2-cyclopentanediol, $cpdH_2$, or *cis*-1,2-cyclohexanediol, $chdH_2$) were studied as models of the formation of Cr(V) complexes with biological 1,2-diols (carbohydrates and glycoproteins) during the reduction of Cr(VI) with biological thiols (e.g., glutathione) in diol-rich biological media.[7,8,16] As shown in Figure 5a,b, the rate of decomposition of the $g_{iso} = 1.9960$ species in dilute ([Cr] = 0.50 mM) DMF solutions was not significantly affected by the presence of a large excess of $cpdH_2$ (1.0 M), but the presence of the diol led to complete replacement of the $g_{iso} = 1.9828$ signal with that of a new Cr(V) species (Cr(V)d in Figure 5b, $g_{iso} = 1.9854$, a Cr(V)−thiolato/diolato complex, see below) and then to a gradual formation of the $g_{iso} = 1.9790$ species (Cr(V)e in Figure 5b, described previously as a Cr(V)−bis-diolato complex, $[Cr^{V}O(cpd)_2]^-$).[16] Similar changes were observed when the concentrated reaction mixture was diluted with DMF containing $chdH_2$ (1.0 M), but in this case, the $g_{iso} = 1.9828$ species were still detectable at the beginning of the reaction (Figure S10b [Supporting Information]). This kinetic behavior could be modeled satisfactorily by the addition of two ligand-exchange reactions to the kinetic scheme (eqs 9 and 10 in Table 2; the ligand concentrations were 1.0 M in all cases and the reactions were treated as pseudo-first-order processes, with the reverse reactions considered negligible).[26] Note that according to the kinetic model (Table 2, eq 9) the diol ligands reacted initially with Cr(V)b ($[Cr^{V}(O)_2(SR)_2]^-$) and not with Cr(V)c ($[Cr^{V}O(SR)_4]^-$). After prolonged reaction times (≥100 min after the dilution at 295 K), when the $g_{iso} = 1.9960$ species were no longer detectable

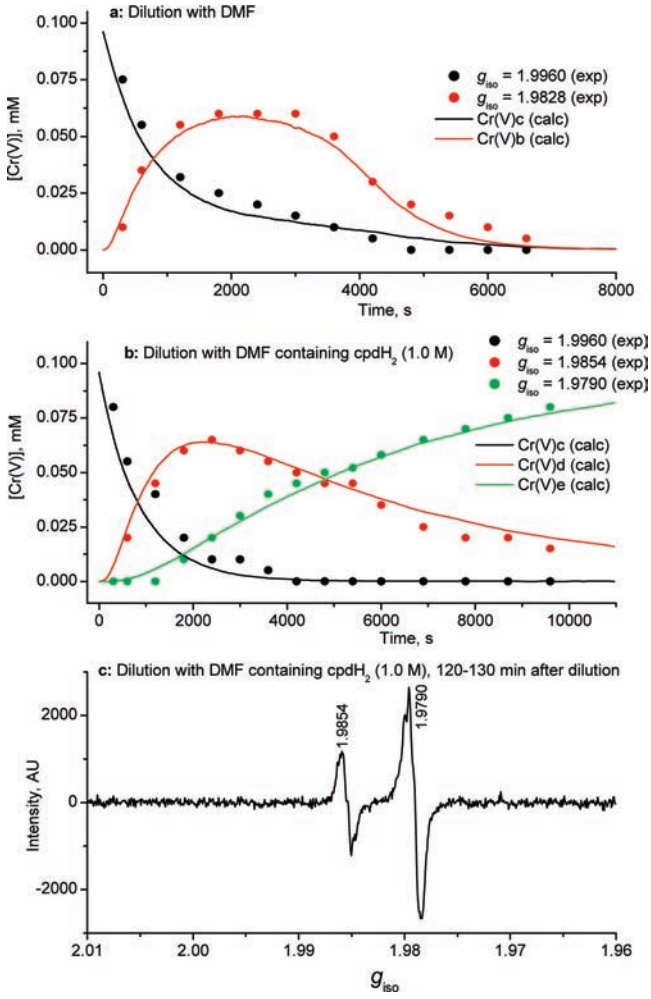

Figure 5. Typical kinetic curves (a, b) and EPR spectra (c) for the decomposition of $[Cr^{V}O(SR)_4]^-$ (g_{iso} = 1.9960 species) in dilute DMF solutions at 295 K in the presence (b, c) or absence (a) of *cis*-1,2-cyclopentanediol (cpdH$_2$, 1.0 M). The $[Cr^{V}O(SR)_4]^-$ complex was generated by the reaction of Cr(VI) (50 mM, from $(NH_4)_2Cr_2O_7$) with RSH (500 mM) in DMF for 15 min at 295 K, then the reaction mixture was diluted 100-fold with an appropriate solvent. Experimental kinetic data (dots in a and b) were obtained by quantitative EPR spectroscopy with $Na[Cr^{V}O(ehba)_2]$ as an internal concentration standard (see the Experimental Section). The EPR spectrum in c was obtained from an average of ten scans in the absence of the Cr(V) standard (the experimental conditions correspond to those in b, reaction time after the dilution 120−130 min). Calculated kinetic curves (lines in a and b) were obtained from the kinetic model in Table 2 (see text for details). Designations of the reaction intermediates (in italics) correspond to Table 2 and Scheme 1.

(Figures 5b and S10b [Supporting Information]), time-dependent EPR spectra of the reaction solutions closely resembled those of Cr(VI)-treated mammalian cells[4,6] or living animals,[5] with the g_{iso} = 1.9854 signal being gradually replaced by that at g_{iso} = 1.9790 (e.g., Figure 5c). Previously,[6] the time-dependent changes in the EPR spectra of Cr(VI)-treated mammalian cells were successfully modeled with a system containing Cr(VI) (0.50 mM), GSH (2.0 mM) and chdH$_2$ (15 mM) in an aqueous buffer solution (pH = 7.4). In a direct reaction of low concentrations of Cr(VI) (0.50 mM) and RSH (5.0 mM) with cpdH$_2$ (1.0 M) in DMF solution, only slow formation of the g_{iso} = 1.9790 species was observed (Figure S10a [Supporting Information]).

The influence of H_2O on the stability of Cr(V)−thiolato complexes and their ligand-exchange products with diols was studied in relation to the likely biological roles of such complexes,[6−9] but the amount of H_2O that could be added to the reaction system was limited by the low water-solubility of RSH (Table S1 [Supporting Information]). Decomposition of the preformed $[Cr^{V}O(SR)_4]^-$ complex after 100-fold dilution with a DMF/H_2O mixture (4:1 vol/vol) was ∼10 times faster than that after the dilution with pure DMF, and led to a ∼3-fold decrease in the amount of the resultant $[Cr^{V}(O)_2(SR)_2]^-$ intermediate (compare Figures 5a and S10c [Supporting Information]). Kinetics of Cr(V) decomposition in H_2O-containing solutions was satisfactorily described (Figure S10c [Supporting Information]) by the general kinetic model of the Cr(VI) + RSH reaction (Table 2), using the rate constants optimized for the DMF/H_2O systems (Table S1 [Supporting Information]). A similar reaction in a DMF/H_2O mixture containing cpdH$_2$ (1.0 M) was characterized (compared with the DMF/cpdH$_2$ system, Figure 5b) by a ∼10-fold increase in the rates of both decomposition of $[Cr^{V}O(SR)_4]^-$ (g_{iso} = 1.9960) and formation of $[Cr^{V}O(cpd)_2]^-$ (g_{iso} = 1.9790), as well as by a ∼5-fold decrease in the amounts of the g_{iso} = 1.9854 intermediate (Figure S10d [Supporting Information]). The optimized kinetic model for this reaction included increases in rate constants k_1 and k_4 (Table S1), as well as increases in the values of k_9 and k_{10} compared with the same reaction in the absence of H_2O (Table 2). In summary, a comparison of kinetic data in Figures 5b and S10d (Supporting Information) showed that the presence of H_2O decreased the stability of Cr(V)−thiolato and Cr(V)−thiolato/diolato complexes, and promoted the formation of Cr(V)−bis-diolato complexes.

To confirm the nature of the g_{iso} = 1.9854 intermediates (Cr(V)d in Figures 5 and S10 [Supporting Information]) as Cr(V)−thiolato/diolato complexes, the same species were generated in higher yields by the reactions of the isolated $K[Cr^{V}OL_2]$ complexes (where L = cpd or chd)[16] with RSH in DMF solutions (Figure 1e and Figure S11 in Supporting Information). Previously, ligand-exchange reactions of $[Cr^{V}OL_2]^-$ with GSH were shown to occur in neutral aqueous solutions.[16] According to EPR spectroscopic data, the maximum yields of the mixed-ligand species were achieved at $[Cr(V)]_0$ = 0.50 mM and [RSH] = 10 mM (Figures 1e and S11b), and ESMS spectra under these conditions were dominated by the $[Cr^{V}OL(SR)_2]^-$ signals (m/z = −543.7 or −557.9 for L = cpd or chd, respectively, Figures 2c and S4f [Supporting Information], and Table 1). Similar to the observations in earlier studies of Cr(V) bis-diolato[16] and 2-hydroxycarboxylato[35] complexes, EPR signals of the $[Cr^{V}OL(SR)_2]^-$ species were fitted by a combination of two signals with close g_{iso} values (Table 1), which were attributed to different geometric isomers (splits in the g_{iso} = 1.9854 signals were obvious from the second-derivative spectra, see the inset in Figure 1e). Unlike for the Cr(V)−bis-diolato complexes,[7,8,16] superhyperfine splitting of the $[Cr^{V}OL(SR)_2]^-$ EPR signals due to the ^{1}H nuclei in the diolato ligands were not resolved. Kinetic studies of the reactions of $K[Cr^{V}OL_2]$ with RSH by electronic absorption spectroscopy (Figure S12 in Supporting Information) confirmed the formation of $[Cr^{V}O(SR)_4]^-$ (λ_{max} ≈ 720 nm, Figure 6) at high concentrations of RSH (e.g., 50 mM at [Cr] = 0.24 mM, Figure S12b [Supporting Information]), and also showed the formation of a spectrally distinct $[Cr^{V}OL(SR)_2]^-$ species (λ_{max} ≈ 550 and 650 nm, Figure 6) at lower RSH concentrations (e.g., 5.0 mM at [Cr] = 0.70 mM, Figure S12a [Supporting Information]). In the both cases, the ligand-exchange reactions were complete within 1−2 min (Figure S12 [Supporting Information]), in contrast to the much slower

(35) (a) Codd, R.; Lay, P. A. *J. Am. Chem. Soc.* **1999**, *121*, 7864–7876. (b) Codd, R.; Lay, P. A. *Chem. Res. Toxicol.* **2003**, *16*, 881–892.

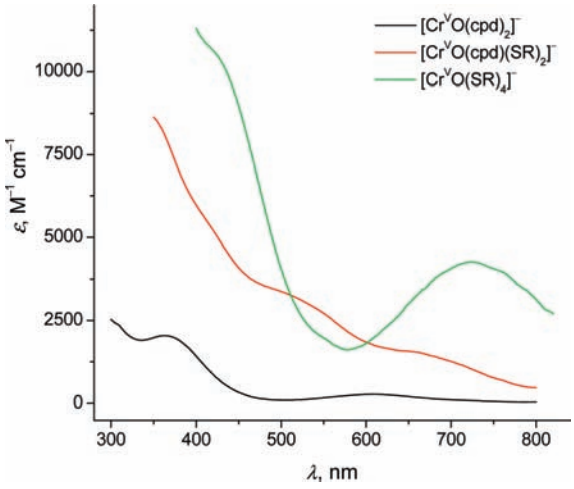

Figure 6. Typical electronic absorption spectra of Cr(V)−bis-diolato,[16] diolato/thiolato and tetrathiolato complexes ($cpdH_2$ = *cis*-1,2-cyclopentanediol; RSH = *p*-bromobenzenethiol). The ϵ values for the $[Cr^{V}O(cpd)(SR)_2]^-$ and $[Cr^{V}O(SR)_4]^-$ complexes were calculated from the time-dependent spectral changes during the reactions of Cr(V)−bis-diolato complexes (~0.5 mM) with RSH (5−50 mM) in DMF solutions (Figure S12 in Supporting Information). The total concentrations of Cr(V) in the reaction solutions were determined by quantitative EPR spectroscopy with $Na[Cr^{V}O(ehba)_2]$ as an internal concentration standard (see the Experimental Section).

reactions of Cr(V)−thiolato complexes with diol ligands (Figures 5 and S10 [Supporting Information]).

Discussion

Mechanisms of the Cr(VI) Reduction Reaction with a Model Thiol. Despite two decades of extensive research into the formation of Cr(V) intermediates during the reduction of Cr(VI) (usually performed by EPR spectroscopy),[7−9,12] mechanistic details of these reactions remain unresolved, largely because of the difficulties with obtaining accurate values of Cr(V) concentrations from EPR spectroscopic data.[8,12,13] In this work, quantitative EPR spectroscopy was applied for the first time for detailed mechanistic analysis of the reaction of Cr(VI) with a simple thiol ligand (RSH = *p*-bromobenzenethiol), used as a model of Cr(VI) reduction by glutathione and other thiols in biological systems.[6,10] The proposed mechanism of Cr(VI) reduction to Cr(III) by excess RSH (Scheme 1) was derived from the following considerations: (i) the known structure[19] of the initial Cr(VI) compound, $[Cr^{VI}(O)_3(SR)]^-$ (Cr(VI) in Scheme 1; could also be formed in situ from $[Cr_2{}^{VI}O_7]^{2-}$ and excess RSH);[11] (ii) the molecular formulas of the Cr(V) intermediates determined by ESMS (Cr(V)b, Cr(V)c, and Cr(V)d in Scheme 1, see also Table 1 and Figure 2); and (iii) the optimized kinetic scheme (Table 2; the equation numbers correspond to those in Scheme 1). The main reaction steps included into Table 2 (and correspondingly into Scheme 1) are explained in detail in the Results section. A similar mechanism, including the formation of organic radicals during the reactions of the organic substrate with a Cr(IV) intermediate, followed by the reaction of these radicals with Cr(VI) to produce Cr(V) intermediates, has been proposed for Cr(VI) reactions with alcohols[24] and 2-hydroxycarboxylic acids[30] in acidic aqueous media. The current work presents the first full modeling of the anomalous kinetic curves for the Cr(V) intermediates[30] that arise from such a mechanism (Figures 4 and S5 [Supporting Information]).

Although the optimized kinetic model (Table 2) did not require an involvement of any Cr(IV) species, the formation of unstable Cr(IV) intermediates (Cr(IV)a and Cr(IV)b, eqs 4 and 6 in Scheme 1) had to be assumed in order to explain the conversion of Cr(V) intermediates into Cr(III) products. One of these species (Cr(IV)a in Scheme 1) corresponds to the $[Cr^{IV}O(SR)_3]^-$ signal observed in ESMS of the reaction mixtures (Figures 2 and S4 [Supporting Information] and Table 1; solvent ligands are usually removed from the complexes under ESMS conditions).[18] Although the appearance of the $[Cr^{IV}O(SR)_3]^-$ signal in ESMS was probably due to the reduction of $[Cr^{V}O(SR)_4]^-$ in the gas phase (see Results),[18] the observation of this species under ESMS conditions supports the existence of small steady-state concentrations of a related Cr(IV) species (Cr(IV)a in Scheme 1) in the reaction solutions. The concentrations of Cr(IV) intermediates in the reaction mixtures, calculated from the kinetic model (Table 2), did not exceed 1% (molar concentration) of the total Cr.

The structures of the Cr(III) products, proposed in Scheme 1 (Cr(III) in eqs 4, 6 and 7) do not correspond to that of the only Cr(III) species observed by ESMS ($[Cr^{III}(SR)_4]^-$ in Table 1 and Figure S4d [Supporting Information]), but its low abundance (Figure S4d) suggests that this is probably a minor product. The Cr(III) products of the Cr(VI) + RSH reaction probably consist mainly of polymeric species (not detected by ESMS), which are formed from Cr(III) monomers containing hydroxido ligands (such as the Cr(III) species in Scheme 1).[36] The polymeric nature of the Cr(III) products is supported by the observed slow (hour time scale at 295 K) formation of a gray-green precipitate during the reactions of Cr(VI) with excess RSH in DMF solutions.

The unusual shapes of the kinetic curves for the formation and decomposition of Cr(V) intermediates (Figures 3 and 4) prevented conventional determination of the rate constants (in contrast to the previous kinetic studies of Cr(VI) reactions with thiols)[31] and warranted full modeling of the observed kinetic curves by the stochastic simulation method (Figures 4 and S5 [Supporting Information]).[26] The optimized kinetic model (Table 2) suggests that the stabilization of Cr(V) species in DMF or DMSO compared with MeCN solutions (Figure 3) occurs through a chain reaction with the participation of solvent free radicals, formed during the reactions of Cr(V/IV) intermediates with the C−H bonds of the solvents (eqs 4 and 5 in Table 2 and Scheme 1). These reactions are likely to be facilitated for DMF or DMSO by the formation of H-bonds between coordinated solvent molecules and oxido groups of the Cr(V/IV) intermediates, while a similar reaction is much less likely in the case of MeCN due to steric considerations (as shown in the last line of Scheme 1). Although stabilization of Cr(V) complexes during the reduction of Cr(VI) in moderately reactive solvents (such as DMF) as opposed to nonreactive ones (such as MeCN)[32] has been noted previously,[24] no mechanistic details of this phenomenon have been described. On the other hand, the presence of highly reactive solvents such as MeOH drastically decreased the lifetime of Cr(V) species (Table S1 and Figure S5 [Supporting Information]).

Some of the modifications of the proposed mechanism (Scheme 1) that were rejected based on the lack of agreement with the observed kinetic data, are presented in Scheme S1 (see also Table S2 and Figure S8, Supporting Information). These include the following: (i) the reaction of a Cr(IV) intermediate with $[Cr^{VI}(O)_3SR]^-$ as the main pathway for regeneration of Cr(V) (instead of the pathway based on solvent radicals, eqs 4 and 5 in Scheme 1); (ii) the formation of a reactive Cr(IV)

(36) Stünzi, H.; Marty, W. *Inorg. Chem.* **1983**, *22*, 2145–2150.

intermediate in the reaction of $[Cr^{V}O(SR)_4]^-$ with RSH, rather than with a solvent molecule (in eq 4, Scheme 1); (iii) the reaction of $[Cr^{V}O(SR)_4]^-$ with $[Cr^{VI}(O)_3(SR)]^-$ as a route for the formation of $[Cr^{V}(O)_2(SR)_2]^-$ during the decomposition of $[Cr^{V}O(SR)_4]^-$; and (iv) the formation of a Cr(IV) species during the reaction of Cr(V)a with RSH in parallel with the formation of Cr(V)b (eq 2 in Scheme 1). Given the high sensitivity of the shapes of the calculated kinetic curves on the reaction mechanism (representative examples are shown in Figure S8 [Supporting Information]), it is unlikely that an alternative kinetic scheme that is consistent with both the observed kinetic data (Figure S5 [Supporting Information]) and the known chemistry of Cr(VI/V/IV) complexes[6] can replace that in Scheme 1.

Three newly described Cr(V) species ($[Cr^{V}(O)_2(SR)_2]^-$, $[Cr^{V}O(SR)_4]^-$, and $[Cr^{V}OL(SR)_2]^-$, where L is a 1,2-diolato(2-) ligand), identified by EPR spectroscopy and ESMS (Table 1), are among the few known Cr(V) complexes with monodentate ligands.[37] Unfortunately, these complexes proved to be too unstable for structural studies (see Results). No crystal structures of Cr(V) complexes with thiolato ligands are known to date,[37] and the only Cr(V)−thiolato complex structurally characterized by X-ray absorption spectroscopy was that with glutathione (where Cr(V) is bound to both thiolato and amido moieties of the ligand).[10] The $[Cr^{V}O(SR)_4]^-$ and $[Cr^{V}OL(SR)_2]^-$ complexes belong to a large group of mono-oxido, five-coordinate Cr(V) complexes (probably of a trigonal bipyramidal geometry),[12,36] and their g_{iso} and A_{iso} (^{53}Cr) values (Table 1) are consistent with those for other Cr(V) complexes of this type.[8,9,12] By contrast, $[Cr^{V}(O)_2(SR)_2]^-$ is a rare example of a four-coordinate, bis-oxido Cr(V) complex, and its A_{iso} (^{53}Cr) value is about half of those for the five-coordinate, mono-oxido Cr(V) species (Table 1).[12] Previously, the A_{iso} (^{53}Cr) values of typical five-coordinate Cr(V) complexes were shown to be lower than those for typical six-coordinate complexes.[12] A related four-coordinate, bis-oxido Cr(V)−amido complex, $[Cr^{V}(O)_2(N^{t}BuAr)_2]^-$ (where Ar = 2,5-C_6H_3FMe) has been isolated and characterized by elemental analyses, NMR spectroscopy and magnetic measurements,[38] but no EPR spectroscopic data for this compound were reported.

Comparison of Cr(VI) Reactions with Glutathione (GSH) and a Model Thiol. A number of features of the Cr(VI) + RSH reactions in nonaqueous solvents, observed in this work, were similar to those found previously for the Cr(VI) + GSH reactions in aqueous solutions.[10] The kinetic profile for the formation and decomposition of a dark-green Cr(V)−GSH intermediate (followed by electronic spectroscopy at 750 nm) during the reaction of Cr(VI) (50 mM) with GSH (500 mM) in aqueous solutions (pH ≈ 7) at 298 K[10] was similar to that for the formation and decomposition of $[Cr^{V}O(SR)_4]^-$ in DMF solutions at the same reagent concentrations (g_{iso} = 1.9960 species, followed by EPR spectroscopy, data set 13 in Figure S5 [Supporting Information]), except that the reaction with GSH was ~20-fold faster.[10] In both cases, the kinetic curves of Cr(V) formation and decomposition were markedly different from those for the intermediates formed in sequential pseudo-first-order reactions.[6,31] The electronic absorption spectrum of this Cr(V)−GSH intermediate (recorded after the dilution of the reaction mixture 100-fold with H_2O)[10] was also similar to that of $[Cr^{V}O(SR)_4]^-$ (Figures 6 and S3 [Supporting Information]), but the visible absorbance band for the former species was less intense and shifted to lower wavelengths (λ_{max} ≈ 630 vs ~720 nm). Dilute solutions of the Cr(VI) + GSH reaction mixtures showed ESMS signals due to $[Cr^{V}O(L'H_3)_2]^-$ (a bis-thiolato−amido chelate complex) and $[Cr^{V}O(L'H_4)_4]^-$ (where $L'H_5$ = GSH),[10] the latter species being a GSH analogue of $[Cr^{V}O(SR)_4]^-$. The existence of an equilibrium between $[Cr^{V}O(L'H_3)_2]^-$ and $[Cr^{V}O(L'H_4)_4]^-$ in the Cr(VI) + GSH system was probably responsible for a much broader EPR signal at g_{iso} ≈ 1.9960 compared with the Cr(VI) + RSH system.[10] Dilute solutions of the Cr(VI) + GSH reaction mixtures showed two main EPR signals (g_{iso} = 1.9960 and 1.9857), and the relative intensity of the latter signal increased with time as the total concentration of Cr(V) species decreased (which mimics the kinetic curves for the g_{iso} = 1.9960 and 1.9828 species in Figure 5a).

Reactions of relatively low concentrations of Cr(VI) (5.0 mM) and GSH (20 mM) in buffered aqueous solutions (pH ≈ 7) led to low total yields of Cr(V) species, and the main Cr(V) signals observed by EPR spectroscopy (particularly at prolonged reaction times) were those at g_{iso} = 1.9857 (A_{iso} (^{53}Cr) = 7.8 × 10^{-4} cm^{-1}).[10,17] The corresponding Cr(V) species could not be detected by ESMS due to the high background signals of GSH ions.[10] The low A_{iso} value (close to that for $[Cr^{V}(O)_2(SR)_2]^-$ but very different from that for the five-coordinate Cr(V) species, Table 1), and the kinetic behavior (similar to that of the g_{iso} = 1.9828 species in Figures 4b and 5a) suggest that the g_{iso} = 1.9857 species observed in the Cr(VI) + GSH system[10,17] are similar to $[Cr^{V}(O)_2(SR)_2]^-$ (g_{iso} = 1.9828, Table 1). The difference in g_{iso} values is likely to be caused by the weak axial binding of either an additional donor group of the ligand (e.g., an amido group in GSH)[10] or a solvent molecule (e.g., H_2O) to the $[Cr^{V}(O)_2(SR)_2]^-$ species, as suggested by the results of experiments with various model thiols.[17,39]

In summary, the two main Cr(V) species (g_{iso} = 1.9960 and 1.9857), formed during the Cr(VI) + GSH reactions in neutral aqueous solutions,[10] are similar in spectral properties and kinetic behavior to the $[Cr^{V}O(SR)_4]^-$ and $[Cr^{V}(O)_2(SR)_2]^-$ complexes (g_{iso} = 1.9960 and 1.9828, respectively, Table 1), formed in the Cr(VI) reaction with a simple model thiol, RSH, in DMF solutions. The same two types of Cr(V)−thiolato species were observed by EPR spectroscopy in Cr(VI) reactions with other model thiols and GSH derivatives in neutral aqueous solutions.[17] Studies of the Cr(VI) reactions with simple model thiols such as RSH in nonaqueous media can partially overcome the practical difficulties in the studies of Cr(V) complexes with GSH or related thiols in aqueous solutions,[10,17] including high reaction rates (which prevent detailed kinetic studies by EPR spectroscopy), low concentrations of the Cr(V) species and difficulties in their detection by ESMS due to the ionic nature of the ligands.

Biological Implications of Cr(V)−Thiolato Complexes. Although most of the kinetic experiments in the Cr(VI) + RSH systems were performed in nonaqueous solutions, the effect of H_2O on the reaction kinetics (which is crucial for the Cr(VI)

(37) Lay, P. A.; Levina, A. In *Comprehensive Coordination Chemistry II*; McCleverty, J. A., Meyer, T. J., Eds.; Elsevier: Oxford, UK, 2004; Vol. 4, pp 313−413.

(38) Odom, A. L.; Mindiola, D. J.; Cummins, C. C. *Inorg. Chem.* **1999**, *38*, 3290–3295.

(39) For instance, two types of Cr(V) intermediates were detected for the reactions of Cr(VI) with *N*-(2-mercaptoethyl)acetamide (R′SH), a non-ionic thiol equally soluble in DMF or H_2O (see ref 11). Similarly to the reactions with RSH (see Results), the $[Cr^{V}O(SR')_4]^-$ species (g_{iso} = 1.9960; A_{iso} ($_{53}$Cr) = 14.6 × 10^{-4} cm^{-1}; *m/z* = −540.0) were generated by the reactions of Cr(VI) (50 mM) with R′SH (500 mM) in DMF solutions, and then the reaction mixtures were diluted 100-fold with either DMF or H_2O. The $[Cr^{V}(O)_2(SR')_2]^-$ species (*m/z* = −320.3) were detected by ESMS in the both solvents, but EPR spectroscopic parameters of these species were solvent-dependent: g_{iso} = 1.9842 (A_{iso} (^{53}Cr) = 7.8 × 10^{-4} cm^{-1}) in DMF solutions; or g_{iso} = 1.9858 (A_{iso} not determined due to the low intensity of the signal) in H_2O solutions (A. Levina, unpublished data).

reactions with thiols in biological media) has also been determined (Table S1 and Figure S5, Supporting Information). Kinetic analysis (Tables 2 and S1 [Supporting Information]) showed that H_2O accelerates the redox reactions of both $[Cr^{VI}(O)_3(SR)]^-$ and $[Cr^{V}O(SR)_4]^-$ (eqs 1 and 4 in Scheme 1), which leads to faster formation and decomposition of Cr(V) species in the presence of H_2O (Figure S5, Supporting Information). Such observations are consistent with the faster reactions observed in the aqueous Cr(VI) + GSH systems.[10] When Cr(VI) is reduced by thiols in fully aqueous media, thiols and their oxidation products can act as the sources of C−H bonds for the formation of organic radicals (eqs 4 and 7 in Scheme 1). This feature is probably responsible for the seemingly paradoxical stabilization of Cr(V)−GSH complexes in neutral aqueous solutions in the presence of high concentrations of GSH.[40] However, in biological systems, other biomolecules such as membrane lipids[41] or the sugar backbone of DNA[42] are more likely to serve as sources of C−H bonds (similar to the structures of the intermediates shown in the last line of Scheme 1), which may lead to the observed stabilization of Cr(V) species in Cr(VI)-treated cultured cells compared with cell-free aqueous solutions.[4]

Another aspect of Cr(V) chemistry in biological systems is the formation of thermodynamically more stable Cr(V) 1,2-diolato complexes (with carbohydrate and glycoprotein ligands) from the initial Cr(V)−thiolato intermediates.[6−8] The current work has demonstrated the unusually slow rates of the ligand-exchange reactions of Cr(V)−thiolato complexes (particularly of $[Cr^{V}O(SR)_4]^-$, Figure 5b) with 1,2-diols in nonaqueous solutions, while the opposite reactions (those of Cr(V)−diolato complexes with thiols) were relatively fast (minutes time scale at 295 K, as shown by electronic spectroscopy, Figure S12 [Supporting Information]). Due to their d^1 electronic structure, Cr(V) complexes are regarded as kinetically labile, so that their ligand-exchange reactions are expected to be complete within seconds at 295 K.[12,37] However, crucially for biological systems, the ligand-exchange reactions of Cr(V)−thiolato complexes with 1,2-diols are drastically accelerated in the presence of H_2O (Figure S10d [Supporting Information]). Therefore, the inefficient replacement of thiolato ligands with diols in nonaqueous media is likely to be caused by the thermodynamic and kinetic barriers for the deprotonation of diols in the absence of H_2O. The other difference between the model system and the *in vivo* chemistry is that the Cr(III) products are most likely to be adducts bound to proteins and DNA[43,44] rather than the insoluble polymers, but this does not affect the redox chemistry involving the higher oxidation states.

The ligand-exchange reactions of Cr(V)−thiolato complexes with cyclic *cis*-1,2-diols (models of carbohydrates, Figures 5b,c and S10 [Supporting Information]) led to EPR spectra that are similar to those of living cells and animals, and respiratory mucus treated with Cr(VI).[4−6,45,46] On the basis of these data, the $g_{iso} \approx 1.986$ and 1.979 signals, observed in Cr(VI)-treated biological systems,[4−6] can be assigned to Cr(V) species of the $[Cr^{V}OL(SR)_2]^-$ and $[Cr^{V}OL_2]^-$ types, respectively (where LH_2 is a biological 1,2-diol and RSH is a biological thiol). An alternative structure of the $g_{iso} \approx 1.986$ species could be $[Cr^{V}(O)_2(SR)_2]^-$ (such as the $g_{iso} = 1.9857$ species observed for the Cr(VI) + GSH reaction in aqueous media, see above), but these species exhibit very narrow EPR signals ($\sim 0.4 \times 10^{-4}$ cm^{-1}),[10] while both the EPR signals observed in Cr(VI)-treated biological media usually have medium widths ($\sim(1-1.5) \times 10^{-4}$ cm^{-1}; such as those in Figure 5c).[4−6] In addition, the kinetics of the ligand-exchange reactions in the Cr(V)−thiolato/diolato systems make the formation of detectable amounts of $[Cr^{V}(O)_2(SR)_2]^-$ in the presence of H_2O and excess diol unlikely (Figure S10e [Supporting Information]). A definitive distinction between $[Cr^{V}(O)_2(SR)_2]^-$ and $[Cr^{V}OL(SR)_2]^-$ on the basis of the A_{iso} values (Table 1) was impossible for biological systems due to the low abundance of the ^{53}Cr isotope.[8,12] Thus, a reaction of Cr(VI) with a simple model thiol, used in this work, has proven extremely useful in the assignment of the nature of Cr(V) species formed in biological systems. These species are likely to act as reactive intermediates in both the Cr(VI)-induced carcinogenesis and the insulin-potentiating activities of Cr(III).[44,47]

Acknowledgment. Financial support of this work was provided by Australian Research Council (ARC) Large and Discovery Grants and Australian Professorial Fellowships to P.A.L. and Wellcome Trust and ARC LIEF Grants for the ESMS and EPR equipment.

Supporting Information Available: (i) Typical examples of experimental and simulated EPR spectra, including those used to check the validity of the calibration method; (ii) typical time-dependent changes in electronic absorption spectra of the Cr(VI) + RSH reaction mixtures; (iii) typical EPR spectroscopic data for the Cr(VI) + RSH + diol reaction mixtures (in addition to those included in Figure 1); (iv) typical ESMS data for the reaction mixtures (in addition to those included in Figure 2); (v) a list of conditions used in kinetic experiments and the corresponding rate constants (k_1, k_4 and k_6, see Table 2); (vi) experimental and calculated kinetic curves for Cr(V) species (obtained by EPR spectroscopy) for all the kinetic experiments; (vii) comparison of calculated kinetic curves for the formation of Cr(V) species under various experimental conditions; (viii) comparison of kinetic data for Cr(V) complexes obtained by EPR and electronic absorption spectroscopies; (ix) typical alternative kinetic schemes (to that shown in Table 2 and Scheme 1) and the corresponding calculated kinetic curves; (x) experimental and calculated stoichiometry of the Cr(VI) + RSH reactions under different conditions; (xi) typical kinetic curves of Cr(V) decomposition in dilute reaction mixtures in the presence or absence of 1,2-diols (in addition to those shown in Figure 5); and (xii) typical changes in electronic absorption spectra during the reactions of Cr(V) diolato complexes with RSH. This material is available free of charge via the Internet at http://pubs.acs.org.

JA101675W

(40) (a) O'Brien, P.; Ozolins, Z. *Inorg. Chim. Acta* **1989**, *161*, 261–266. (b) O'Brien, P.; Pratt, J.; Swanson, F. J.; Thornton, P.; Wang, G. *Inorg. Chim. Acta* **1990**, *169*, 265–269.
(41) (a) Schaich, K. M. *Lipids* **1992**, *27*, 209–218. (b) Malle, E.; Marsche, G.; Arnhold, J.; Davies, M. J. *Biochim. Biophys. Acta* **2006**, *1761*, 392–415.
(42) Levina, A.; Barr-David, G.; Codd, R.; Lay, P. A.; Dixon, N. E.; Hammershøi, A.; Hendry, P. *Chem. Res. Toxicol.* **1999**, *12*, 371–381.
(43) Macfie, A.; Hagan, E.; Zhitkovich, A. *Chem. Res. Toxicol.* **2010**, *23*, 341–347.
(44) Levina, A.; Lay, P. A. *Chem. Res. Toxicol.* **2008**, *21*, 563–571.
(45) Codd, R.; Lay, P. A. *J. Am. Chem. Soc.* **2001**, *123*, 11799–11800.
(46) Codd, R.; Lay, P. A.; Tsibakhashvili, N. Ya.; Kalabegishvili, T. L.; Murusidze, I. G.; Holman, H.-Y. N. *J. Inorg. Biochem.* **2006**, *100*, 1827–1833.
(47) (a) Levina, A.; Mulyani, I.; Lay, P. A. In *The Nutritional Biochemistry of Chromium(III)*; Vincent, J. B., Ed.; Elsevier: Amsterdam, 2007; pp 225−256. (b) Mulyani, I.; Levina, A.; Lay, P. A. *Angew. Chem., Int. Ed.* **2004**, *43*, 4504–4507. (c) Nguyen, A.; Mulyani, I.; Levina, A.; Lay, P. A. *Inorg. Chem.* **2008**, *47*, 4299–4309.